Constituent-interchange model for inclusive vector-meson production

Kashyap V. Vasavada
Department of Physics, Indiana-Purdue University, Indianapolis, Indiana 46205
(Received 14 July 1978)

The constituent-interchange model is applied to inclusive vector-meson production in proton-proton collisions. In particular, production of ψ, ψ', and ρ mesons is considered and good agreement with all the distributions is obtained.

I. INTRODUCTION

Models based on quark-partons have been extensively considered recently for high-energy reactions. In particular, the constituent-interchange model (CIM), in which a quark-parton from one particle interacts with a meson or baryon constituent of the other particle, has been very successful in dealing with large-transverse-momentum (Q_T) processes.[1] In a recent paper[2] Blankenbecler, Duong-Van, and the author have applied this model to massive-lepton-pair production for the entire Q_T range. It was found that the CIM gives a correct gauge-invariant extension of the Drell-Yan model[3] and automatically gives rise to large-Q_T dileptons without assuming large transverse momentum of the initial partons (K_T). That work dealt mainly with the continuum and, although very good agreement was obtained for an extensive range of Q_T and Q^2 (mass^2 of dimuon), the overall normalization had to be readjusted for low Q^2 and especially in the resonance region (ψ). In another paper[4] the author considered angular distributions of muons in various theoretical models including CIM. The present work is a natural extension of these ideas to vector-meson production which contains a large part of the dilepton production cross section. Most of the time we will consider dimuon resonant production data. But it is clear that the cross-section equations are readily applicable to the production of other decay products of the same resonances when the corresponding branching ratios are used. For the present we will consider production of $\psi(3.1)$, $\psi'(3.7)$, and $\rho(0.770)$ mesons in proton-proton collisions. Production of other vector mesons and reactions involving different incident beams will be considered later. It turns out that the model fits the extensive set of data rather well for the entire range of kinematic variables in each case.

Since the discovery of ψ production in hadronic collisions, a number of authors have considered various models. They include generalized Drell-Yan models or quark-fusion models with charmed quarks[5] and normal quarks[6] and also gluon-fusion models.[7] For the ρ production, to our knowledge, complete parton-model calculations have not appeared in the literature.[16] In Sec. II we describe the model. Numerical results for distributions are given in Sec. III and coupling constants are discussed in Sec. IV. Section V contains concluding remarks.

II. DETAILS OF THE MODEL

In the CIM picture [Fig. 1(a)] the hadrons A and B emit partons[8] (quark a and meson b and vice versa) which then undergo a hard scattering to produce the vector meson Q and the quark d. Fig-

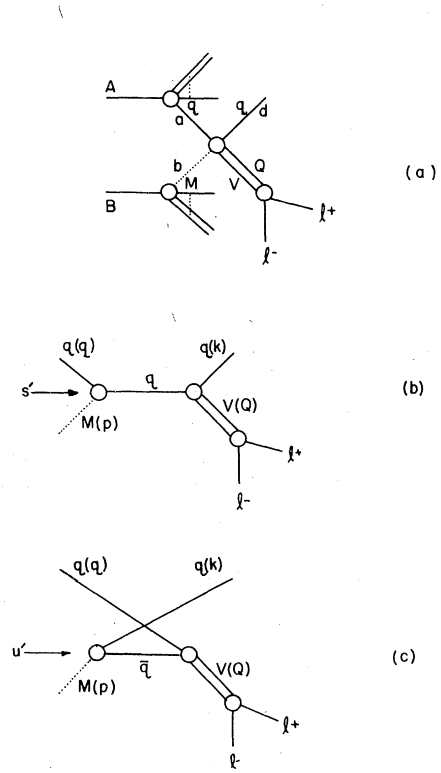

FIG. 1. (a) CIM diagram for dilepton production in the resonance region. (b) s-channel pole for the subprocess: quark + meson → quark + vector meson (dilepton). (c) u-channel pole for the same subprocess.

ures 1(b) and 1(c) show the two leading s- and u-channel q- ($\bar{q}$-) exchange diagrams which would make the amplitude gauge invariant when Q is a photon and b is a π^0 meson. The u-channel diagram involves quark-antiquark annihilation and is clearly related to the Drell-Yan model for the process. The fully differential cross section is given by

$$\frac{d^4\sigma}{d^4Q}(AB \to l^+l^- X) = \sum_{a,b,d} \int_0^1 dx_1 \int_0^1 dx_2 G_{a/A}(x_1) G_{b/B}(x_2) \frac{d^4\sigma}{d^4Q}(ab \to l^+l^- d) . \tag{1}$$

Here G's are the usual probability functions for finding a and b in the hadrons with four momenta $-x_1P_A$ and x_2P_B, respectively. Transverse momenta of a and b are regarded as small and the dependence is suppressed in the equation. As in Ref. 2 an average value ($\langle K_T \rangle$) can be added later if desired. The differential cross section for the subprocess is readily obtained by summing over the Feynman diagrams [Figs. 1(b) and (c)] and is given by

$$\frac{d^4\sigma}{d^4Q}(ab \to l^+l^- d) = \frac{R}{(Q^2 - m_V^2)^2 + m_V^2\Gamma^2} , \tag{2}$$

where

$$R = \frac{g_{Vl^+l^-}{}^{-2} g_{Vq\bar{q}}{}^2 h^2}{96\pi^4} \Sigma(s', t', u') \delta(s' + t' + u' - Q^2 - m_a{}^2 - m_b{}^2 - m_d{}^2) , \tag{3}$$

$$s'\Sigma = \frac{\lambda^2(u', Q^2, m^2)}{(m^2 - u')^2} + \frac{\lambda^2(s', Q^2, m^2)}{(s' - m^2)^2} + \frac{2}{(s' - m^2)(m^2 - u')} [2Q^2(s' - Q^2 + u') + (s' - Q^2 - m^2)(u' - Q^2 - m^2)] , \tag{4}$$

and

$$\lambda^2(a, b, c) = a^2 + b^2 + c^2 - 2(ab + bc + ca) . \tag{5}$$

s', t', u' are the usual Mandelstam variables for the subprocess. h is the meson-quark-antiquark coupling constant used in Ref. 2. Its value is obtained by a CIM fit to the large-p_T production of π mesons. The latter fit gives the 90° meson-quark scattering differential cross section by

$$\frac{d\sigma}{dt}(Mq \to Mq) = c/s^4 \tag{6}$$

with $c = 1200$ GeV^4. h^2 is then given by $\sqrt{16\pi c}$. The uncertainties in this number are believed to be of the order of a factor of 2 or so. $g_{Vl^+l^-}{}^{-2}$ is obtained from the partial width of v to l^+l^- channel:

$$\Gamma(V \to l^+l^-) = \frac{1}{3} \frac{g_{Vl^+l^-}{}^{-2}}{4\pi} m_V . \tag{7}$$

m is the effective mass of the quark and is taken to be 1 GeV as in Ref. 2 (except in the case of ρ production as will be discussed in the following). Hence the only unknown in the present work is the coupling of V to the quarks ($g_{Vq\bar{q}}$).

For comparison with experiments we do the Q^2 integration over the Breit-Wigner shape. The total cross section (into l^+l^-) is obtained by d^4Q integration, which gives,[9] for $A \equiv B$,

$$\sigma(s) = 2 \int_0^1 dx_1 \int_0^1 dx_2 G_{a/A}(x_1) G_{b/B}(x_2) \times \sigma(ab \to l^+l^- d) , \tag{8}$$

where

$$\sigma(ab \to l^+l^- d) = \frac{g_{Vl^+l^-}{}^{-2} g_{Vq\bar{q}} h^2}{384\pi^2 s'^2} \frac{\lambda(s', Q^2, m^2) F(s')}{m_V \Gamma} \tag{9}$$

and

$$F(s') = \frac{\lambda^2(s', Q^2, m^2)}{(s' - m^2)^2} + \frac{Q^2(Q^2 - 4m^2)}{4p^2k^2} \frac{1}{z^2 - 1} - \frac{2Q^2}{s' - m^2} - 1 + \left(4Q^2 + \frac{2Q^2(4m^2 - Q^2)}{s' - m^2}\right) \frac{1}{4pk} \ln \frac{z + 1}{z - 1} , \tag{10}$$

with

$$z = \frac{2p_0k_0 - M^2}{2pk} . \tag{11}$$

In the above, p_0, p and k_0, k are, respectively, the energy and three-momentum of the initial meson and final quark in the c.m. system of the two-body subprocess ($a + b \to Q + d$). M is the mass of the meson (note that the notation has been slightly changed from Ref. 2).

The factor of 2 in Eq. (8) arises from the two diagrams with a = meson and b = quark and vice versa. For $A \neq B$, one has to exchange a and b explicitly. The summation sign over a, b, d is dropped from now on. Different quarks will be taken into

account by explicit multiplication of the G function by a numerical factor, and the different mesons will be included by using one effective G function for the entire class of mesons. d forms part of "anything" with probability 1 in the inclusive cross section.

We have the usual meaning for the other kinematic variables. w is the overall proton-proton c.m. energy ($s=w^2$), y and X are, respectively, the c.m. rapidity and Feynman scaling variable $Q_L/Q_{\max}$. The distributions $d\sigma/dy$, $d\sigma/dX$, $Q_0 d^3\sigma/d^3Q$, $d\sigma/dQ_T{}^2$ can be obtained by doing one of the x integrations with the help of the δ function in (3) and then integrating over the other independent variables. B will denote the branching ratio into $\mu^+\mu^-$ (μ-e universality is assumed).

The probability functions are taken to be as follows[10]: For an up quark in the proton

$$G_{u/p}(x) = \frac{0.2(1-x)^7}{x} + \frac{1.89(1-x)^7}{\sqrt{x}} + \begin{cases} 90.2x^{3/2}e^{-7.5x}, & x \le 0.35 \\ 5(1-x)^3, & x \ge 0.35 . \end{cases} \quad (12)$$

The down quarks in the proton could have a different distribution, but the difference is not crucial here. They can be simply included by considering the fact that there are two up quarks and one down quark in the proton. For a meson in the proton we have

$$G_{M/p}(x) = 0.2(1-x)^5/x . \quad (13)$$

For charmed quarks or antiquarks we take the sea-type distribution given by the dimensional-counting rules

$$G_{c/p}(x) = G_0(1-x)^7/x . \quad (14)$$

$G_{M/p}(x)$ was determined in Ref. 2 by requiring it to satisfy the sum rule

$$G_{\bar{q}/p}(x) = \int_x^1 \frac{dw}{w} G_{\bar{q}/M}\left(\frac{x}{w}\right) G_{M/p}(w) . \quad (15)$$

For ψ production we consider a (or b) to be either a normal (up or down) quark or a charmed quark. For ρ production they will be taken to be normal quarks. In the next section we discuss various distributions.

III. DISTRIBUTIONS

As we have already mentioned, all the parameters, with the exception of $g_{V\bar{q}\bar{q}}$, have been already determined in the previous work.[2] This is fixed by requiring agreement with one data point. All the other distributions are then predictions. Numerical values of these coupling constants will be discussed in the next section.

A. $\psi(3.1)$ production

We have studied this process in detail over a wide range of kinematic variables. Data are taken from Refs. 11 and 12. Some of the results are shown in Figs. 2–6. The solid curves represent our calculation with normal quarks [$G(x)$ given by Eq. (12)]. The dotted curves are obtained when a or b (and hence d) is a charmed quark or antiquark with $G(x)$ given by Eq. (14), and the coupling constant is suitably adjusted. The dashed curves are obtained for normal quarks with a $(1-x)^4$ distribution (discussed below).

Figure 2 shows dependence of σ on w. The agreement is good for the normal quark model except for the very highest CERN ISR point. The threshold behavior is well reproduced. In addition, we found that the slope can be increased for high w by using a very large quark mass m. But, for the figures shown, m has been taken to be 1 GeV as in Ref. 2.

Figure 3 shows $Bd\sigma/dy|_{y=0}$ vs w. Here again the agreement is good.

Figure 4 shows $Bd\sigma/dX$ vs X for $w=20.8$ GeV. Here the solid curve (a) is calculated with previous functions and parameters. At higher values of X

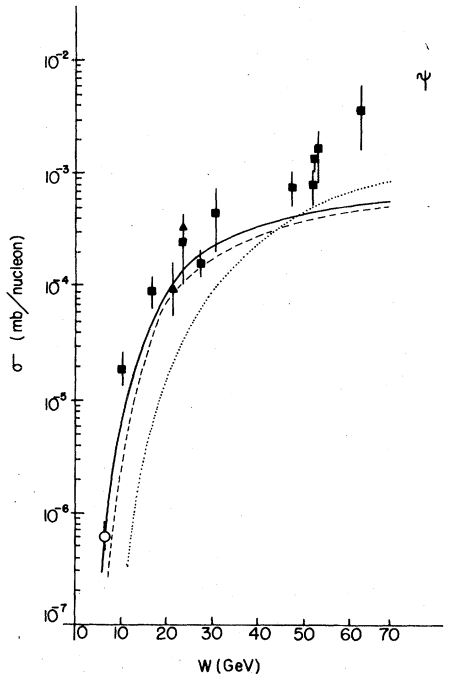

FIG. 2. Predicted total cross sections $\sigma(\psi)$ at various c.m. energies with data taken from Ref. 11. The solid curve is for the normal quark model with x distribution given by Eq. (12), and the dashed curve is for the same model with $(1-x)^4$ distribution explained in the text. The dotted curve is for the charmed-quark model with sea distributions.

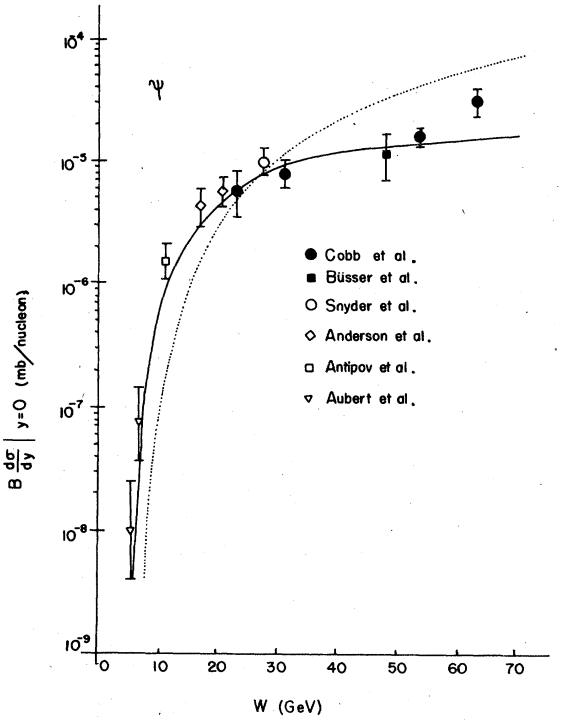

FIG. 3. Predicted differential cross sections at $y=0$ for various c.m. energies. Data are taken from Ref. 12. The solid curve is for the normal quark model. The dotted curve is for the charmed-quark model with sea distributions.

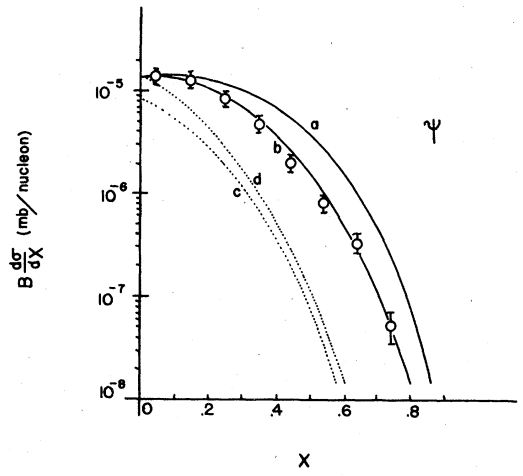

FIG. 4. Predicted Feynman-X distributions. Curve (a) is obtained with standard functions and parameters. Curve (b) is obtained with $G_{u/p}(x) \propto (1-x)^4$ as $x \to 1$. Curve (c) represents charmed-quark model with sea distributions. Curve (d) is obtained from (c) by readjusting the normalization at $X=0$ independently of the other distributions. Data are taken from Anderson *et al.*, Ref. 12 ($E_{\text{inc}}=150$ GeV).

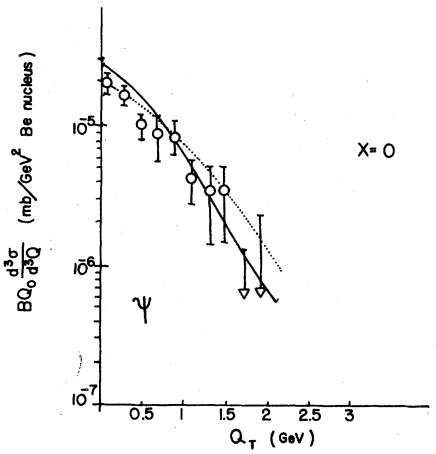

FIG. 5. Predicted inclusive cross sections for various transverse momenta. The solid curve is for the normal quark model and the dotted curve is for the charmed-quark model. Data are from Snyder *et al.*, Ref. 12 ($E_{\text{inc}}=400$ GeV).

(say ~0.6), predicted values are larger by about a factor of 3 or so. This implies that the G's should fall slightly more strongly at high X. So we changed $(1-x)^3$ in Eq. (12) to $(1-x)^4$ and obtained curve (b) which agrees completely with data. The effect of this change on other figures will be discussed below. The dotted curve (c) is obtained for the charmed-quark model by taking $G_{c/p}(x)$ from Eq. (14). If we adjust the normalization of this curve at $X=0$ independently of the other figures, then curve (d) is obtained. In either case these curves are just too steep. Even at not too large X (around $X \sim 0.6$) they give $Bd\sigma/dX$ smaller than the

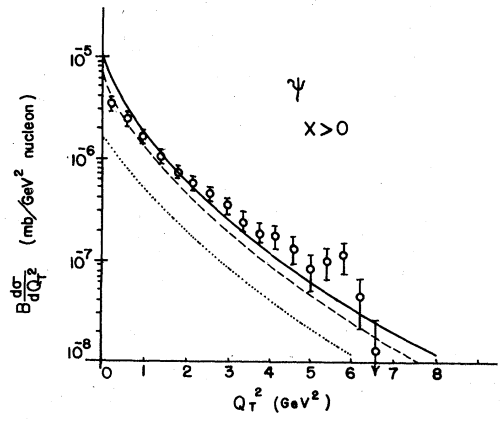

FIG. 6. Predicted transverse-momentum distribution. The solid curve is for the normal quark model with x distribution given by Eq. (12), and the dashed curve is for the same model with $(1-x)^4$ distribution. The dotted curve is for the charmed-quark model. Data are taken from Anderson *et al.*, Ref. 12 ($E_{\text{inc}}=150$ GeV).

data by a factor of about 40 to 70. Such a disagreement has been also found previously in the Drell-Yan or quark-fusion models for ψ production with charmed quarks having sea distributions.[5] Such a model then should be ruled out completely regardless of any ambiguities in the coupling constants. Of course, if one gives charmed quarks valence-type distributions, agreement can be obtained with data since then there is very little difference from the normal quark model presented above. This will be similar to the quark fusion model of Donnachie and Landshoff.[5] However, it should be noted that recent large-Q^2 data on dilepton production[13] give $G(x) \propto (1-x)^N$ (with N ranging from 7 to 10 depending on various scale-breaking assumptions) for sea quarks and hence flat sea distributions are ruled out. Moreover, electroproduction data[14] and ratios of particles produced at large p_T in p-p collisions[15] also tend to make flat sea distributions unacceptable.

In Figs. 5 and 6 we show $BQ_0 d^3\sigma/d^3Q$ vs Q_T and $Bd\sigma/dQ_T{}^2$ vs $Q_T{}^2$. The agreement is again good. Some deviation at small Q_T is presumably due to the neglect of small k_T fluctuations in the initial state. These fluctuations can be seen to lower the theoretical curve, in agreement with the data

The changes brought about by taking $(1-x)^4$ instead of $(1-x)^3$ distribution in Eq. (12) for our model are shown by dashed curves. It can be seen that there are small changes in Fig. 2 (σ vs w) and Fig. 6 ($d\sigma/dQ_T{}^2$ vs $Q_T{}^2$). The corresponding dashed curves obtained for Fig. 3, and Fig. 5 are indistinguishable from the solid curves and hence are not shown. Thus for all the distributions the agreement remains reasonable even with the modified $(1-x)^4$ behavior.

B. $\psi'(3.7)$ production

The ψ' production data are still very meager and the errors are large. We adjust the coupling constant $g_{\psi' q\bar{q}}$ by requiring agreement with $Bd\sigma/dy|_{y=0}$ for $E_{\rm inc}=400$-GeV data (Snyder *et al.*, Ref. 12). Other cross sections are then predicted. For example, the predicted and experimental values of $B\sigma(\psi')$ at $E_{\rm inc}=400$ GeV are 0.184 ± 0.092 and 0.191 ± 0.142, respectively. Hence the agreement is good. From data by Branson *et al.* (Ref. 12) for $E_{\rm inc}=225$ GeV, we have

$$\left.\frac{B\sigma(\psi')}{B\sigma(\psi)}\right|_{\rm expt} = 0.007 \pm 0.004 ,$$

while the predicted values are 0.015 ± 0.011. So again the predicted value agrees with the experimental value within uncertainties.

C. ρ (0.770) production

Extensive ρ production data have become available recently.[12,16] Figures 7–11 show results of our

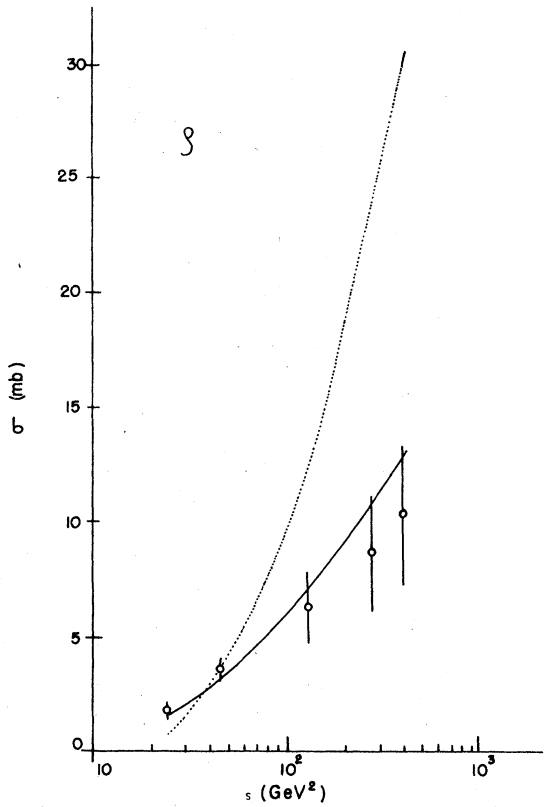

FIG. 7. Predicted total cross section $\sigma(\rho)$ for various s. The solid curve is for the quark mass $m=0.47$ GeV. The dotted curve is for $m=1$ GeV. Data are taken from the compilation by Bockmann, Ref. 16.

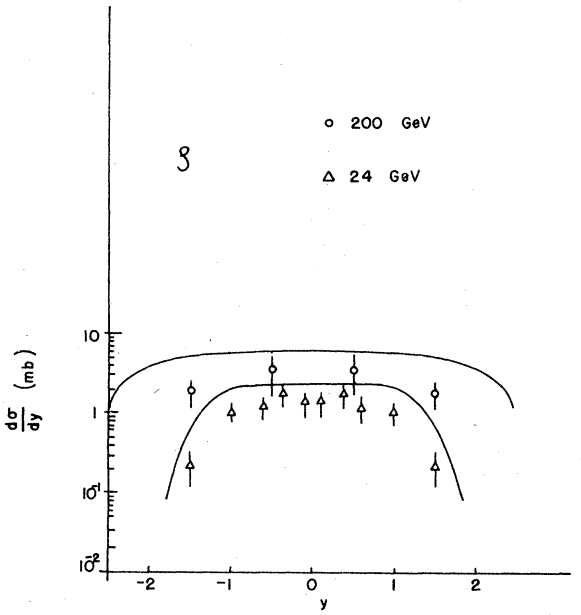

FIG. 8. Predicted c.m. rapidity distribution. The top and the bottom curves are for $E_{\rm inc}=200$ GeV and 24 GeV, respectively. The data are from the compilation by Bockmann, Ref. 16.

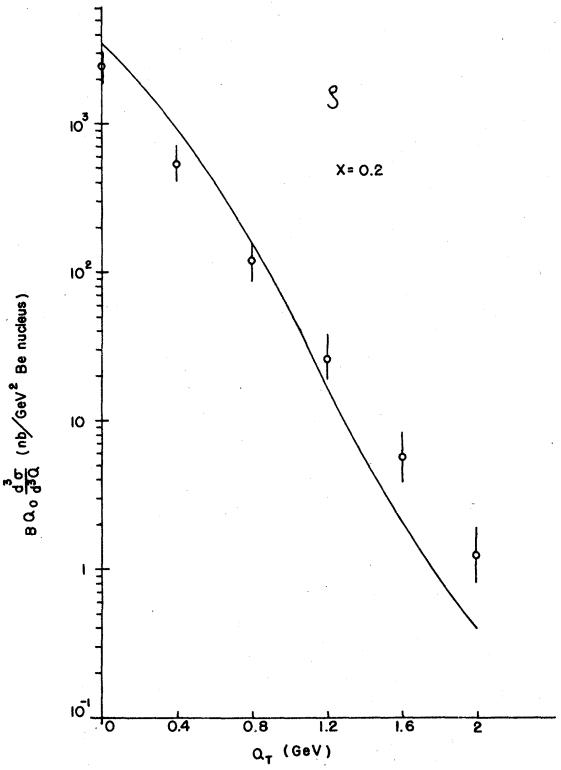

FIG. 9. Predicted inclusive ρ production cross section for various transverse momenta. Data are taken from Anderson *et al.*, Ref. 12 (E_{inc} = 150 GeV).

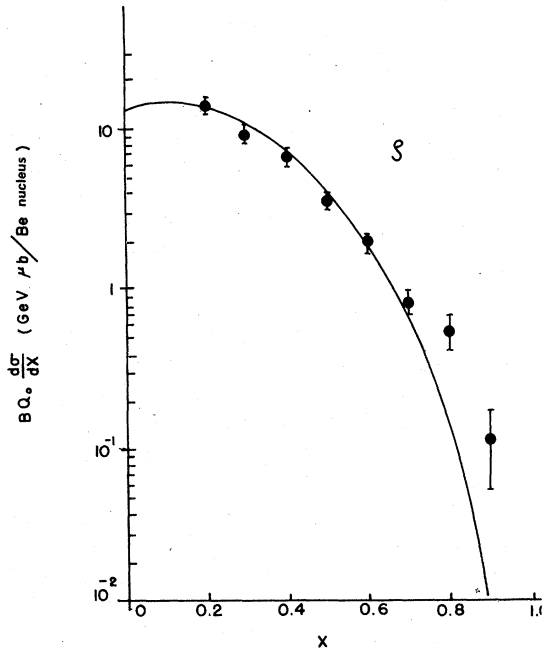

FIG. 10. Predicted Feynman-X distribution. Data are from Anderson *et al.*, Ref. 12 (E_{inc} = 150 GeV).

calculation. If we keep the effective quark mass m as 1 GeV as in the ψ production, the dotted curve in Fig. 7 (σ vs s) is obtained by normalizing at $s = 46.9$ GeV^2. Thus the energy dependence is clearly wrong. Hence the effective mass was changed to 0.47 GeV and the solid curve was obtained. The question of quark mass will be discussed shortly. In the meantime note that all the rest of the curves were obtained with the same quark mass, and the coupling constant $g_{\rho q\bar{q}}$ was obtained by requiring agreement at $s = 46.9$ GeV^2 for σ. Figures 8–11 show $d\sigma/dy$ vs y, $BQ_0 d^3\sigma/d^3Q$ vs Q_T, $BQ_0 d\sigma/dX$ vs X, and $(B/Q_T)(d\sigma/dQ_T)$ vs Q_T. The agreement is reasonable. All the curves are shown for the normal quark distribution $G_{u/p}(x)$ from Eq. (12).

Now, the question of quark masses is a subtle one. One problem in extending models like CIM from high-Q_T, high-Q^2 to low-Q_T and/or low-Q^2 region is that the results do become sensitive to the masses. In fact, for zero mass (or even small mass in some cases) poles start appearing in the physical region. In the ψ-ψ' case the intermediate and final quark masses in the Feynman diagrams were taken as 1 GeV from our previous work[2] on continuum μ pair production at large Q^2. This is

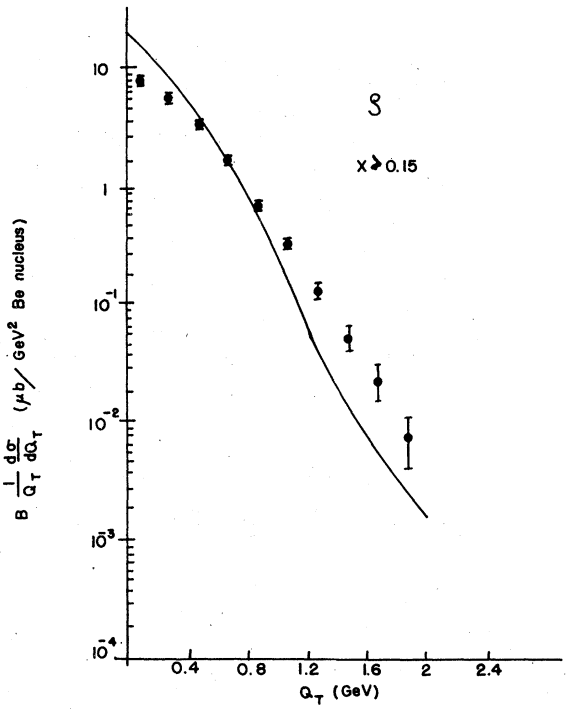

FIG. 11. Predicted transverse-momentum distribution. Data are taken from Anderson *et al.*, Ref. 12 (E_{inc} = 150 GeV).

just regarded as some effective quark mass. In absence of an understanding of quark binding, one can hardly insist that the effective mass must be the same as the spectroscopic quark mass. In the ρ-meson case, $m=1$ GeV did not give the correct energy dependence but $m=0.47$ GeV gave it very well. Hence for all the ρ distributions the latter value was chosen. In the ψ-meson case $m=0.47$ GeV, however, does give rise to wrong shapes of the curves. Although this was forced on us by the data, it does not seem surprising that the effective quark mass in the ρ production comes out to be smaller than that in the case of heavier ψ-ψ' production. Heavier states can be more easily formed by heavier effective constituent masses. It is likely that the quark masses in our calculation play a role similar to the cutoffs in field theories. As a matter of fact, models like quantum chromodynamics do need cutoffs when they are extended to low Q_T. It would be indeed meaningless if it were necessary to have different effective masses for different kinematic regions of production of the same states. But this was certainly not the case. For the present then, we regard the necessity of heavier effective masses for production of heavier states as intuitively acceptable, although deeper understanding will be desirable. In the following section we discuss the numerical values of the coupling constants required by the data.

IV. COUPLING CONSTANTS

We have not considered charges or colors explicitly. So our couplings $g_{Vq\bar{q}}{}^2$ will be averages over these quantum numbers. For ψ production with normal quarks, we find from the distributions,

$$\frac{g_{\psi q\bar{q}}{}^2}{4\pi}=4.7\times10^{-3} \tag{16}$$

with about 40% uncertainty. One way to get an idea of the size of this coupling is to look at the ratio of normal hadrons to muons produced in e^+-e^- collisions in the ψ region. We have

$$\frac{g_{\psi q\bar{q}}{}^2}{4\pi}=R\,\frac{g_{\psi\mu^+\mu^-}{}^2}{4\pi}\,, \tag{17}$$

where

$$R=\frac{\Gamma(\psi\to\text{normal hadrons})}{\Gamma(\psi\to\mu^+\mu^-)}\simeq 12\,.$$

This gives

$$\frac{g_{\psi q\bar{q}}{}^2}{4\pi}=5.6\times10^{-5}\,. \tag{18}$$

Thus the value obtained in the present work is larger than the value given by e^+e^- data by a factor of about 80. The constants of Ref. 2 can, however, be increased by a factor of 2 or so and still provide a good fit to the continuum data. So the discrepancy could be reduced to a factor of about 40. In addition, we have noticed that in the present model, a smaller quark mass is generally accompanied by a smaller coupling constant to fit the data. For example, reducing m to 0.35 GeV would reduce the required coupling $g_{\psi q\bar{q}}{}^2$ by a factor of 12. In any case, there is some discrepancy in the values of the couplings obtained in the two processes.

Some previous authors[5] who considered ψ production in Drell-Yan or quark-fusion models have been led to reject the role of normal quarks because of such a small size of the coupling constant. However, it seems to us that this may be premature in the absence of good understanding of quark confinement and the mechanism of the Okubo-Zweig-Iizuka (OZI) rule violation. As is generally believed, ψ and ψ' have charmed quarks as their main components. Hence ψ-ψ' couplings to normal quarks are OZI-rule-violating couplings. The major contribution in the ψ production process comes from the u-channel graph [Fig. 1(c)] in which at least one of the quarks in the $\psi q\bar{q}$ vertex is highly off mass shell (in fact, spacelike). For the ψ decay into hadrons in e^+e^- annihilation, the quarks will be timelike. The OZI rule and the magnitude of OZI-rule-violating couplings are still controversial and ill understood.[17] Hence it is possible that there is a large variation in going from timelike to spacelike region.[18] Moreover, our $\psi q\bar{q}$ vertex probably already contains renormalization effects due to gluon exchanges. These corrections could depend on the off-mass-shell or on-mass-shell nature of the particles involved. Such effects could also account for the different effective quark masses found in fitting the ψ and the ρ production. In current algebra, difficulties with such large extrapolations are well known. In connection with Regge pole couplings also large variations in going from spacelike to timelike regions are often found.[19] So in the present context such a variation cannot be ruled out at present. Note that all the distributions look very similar to the continuum μ pair production. This fact would hint at a similar dynamics. Because of these reasons, we regard the normal quark production of ψ as still a viable model. The size of the coupling would remain as an outstanding problem.

Another way to get some idea of the magnitude of $Vq\bar{q}$ or $Vc\bar{c}$ coupling is through the vector-dominance model of Fig. 12. Assuming saturation one finds

$$g_{Vq\bar{q}}=g_V=\frac{e^2}{g_{V\mu\mu}}\,, \tag{19}$$

with a similar equation for $c\bar{c}$. Applying the saturation procedure to $\psi q\bar{q}$, one finds $g_{\psi q\bar{q}}{}^2/4\pi=11.7$ using Eq. (7) for $\Gamma(\psi\to\mu^+\mu^-)$. For $\psi q\bar{q}$, however, this

saturation is unjustified since other low-mass vector mesons like ρ will surely contribute to Fig. 12(a). On theother hand, for $\psi c\bar{c}$, the saturation may be correct since presumably no other low-mass vector meson has appreciable coupling to $c\bar{c}$. Then we have

$$\frac{g_{\psi c\bar{c}}^{2}}{4\pi} = 11.7. \tag{20}$$

Now our fits in the last section require $G_0 g_{\psi c\bar{c}}^{2}/4\pi = 0.044$. Not much is known about G_0 for charmed quarks in the nucleon. So $g_{\psi c\bar{c}}^{2}/4\pi$ can be made to agree with the vector-dominance value in (20) by choosing G_0 to be 0.0037. Various authors have chosen values of G_0 ranging from very small to quite large.[5] But, as we have already mentioned, the charmed-quark model (with sea-type distributions) has difficulties more serious than the coupling constants. One problem, not mentioned before, is the associated production of charmed particles. Experimentally this seems to be suppressed[20] ($\sigma_{\psi c\bar{c}}/4\pi < 1\%$), and, unless G_0 is extremely small, $\sigma_{\psi c\bar{c}}$ would come out to be relatively large in the $c\bar{c}$ model. This, however, is a highly model-dependent question.

Turning now to the ψ' coupling, we find that our fits require

$$\frac{g_{\psi' q\bar{q}}^{2}}{4\pi} = 1.1\times 10^{-3} \tag{21}$$

with about 70% uncertainty, while a calculation involving the ratio of normal hadrons to $\mu^+\mu^-$ in ψ' region of e^+e^- annihilation gives

$$\frac{g_{\psi' q\bar{q}}^{2}}{4\pi} = 1.7\times 10^{-4}. \tag{22}$$

So, although there is some discrepancy, curiously, it is much smaller than in the ψ case. This coupling is also OZI-rule violating, and the same remarks as in the case of ψ apply here.

As for the ρ coupling, the fits require (with $m = 0.47$ GeV)

$$\frac{g_{\rho q\bar{q}}^{2}}{4\pi} = 1.9 \tag{23}$$

with about 15% uncertainty. Applying vector dominance we find

$$g_{\rho q\bar{q}} = g_{\rho} = g_{\rho\pi\pi}, \tag{24}$$

and hence

$$\frac{g_{\rho q\bar{q}}^{2}}{4\pi} = \frac{g_{\rho\pi\pi}^{2}}{4\pi} = 2.3. \tag{25}$$

This is also approximately consistent with the value obtained from $\Gamma(\rho \to \mu^+\mu^-)$. Thus the ρ coupling is in good agreement with the vector-dominance value. This may be a reflection of the fact that

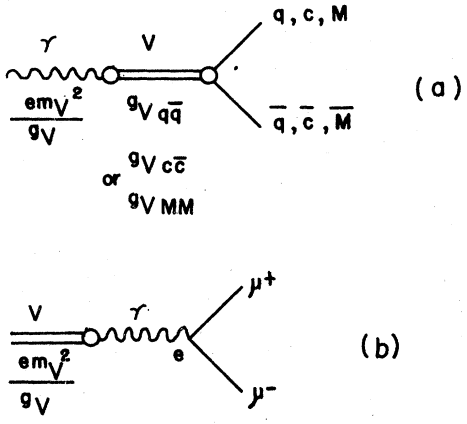

FIG. 12. Vector-dominance model for coupling constants.

$\rho q\bar{q}$ is allowed by OZI rule, and variation from timelike to spacelike region may be moderate.

V. CONCLUDING REMARKS

In the present work we extended our previous CIM for continuum μ pair production to vector-meson production in proton-proton collisions. For ρ production the results were very good. Agreement with nearly all distributions was obtained with an OZI-rule-allowed coupling constant $g_{\rho q\bar{q}}$ consistent with the vector-meson-dominance model. In fact, considering that there could be many other diagrams, it is somewhat surprising that the CIM does well in widely different kinematic regions. Presumably many of such effects are automatically included. For ψ production good fits to the distributions were obtained but with a coupling constant larger than that suggested by the decay of ψ into hadrons. Plausible reasons were discussed in the previous section. Difficulties with the charmed-quark model for ψ production were also discussed.

In view of the simplicity of the model detailed χ^2 fits were not attempted. In both ψ and ρ production, the couplings were adjusted such that agreement was obtained with one data point in each case. These data values themselves have uncertainties of at least 30 to 40%. In addition, it should be kept in mind that the experiments themselves have some ambiguities, various cuts and acceptance problems. Thus, on the whole, the agreement should be regarded as good.

Several authors[7] have considered gluon fusion to produce χ which subsequently decays into ψ and γ. Gluon distributions are not *a priori* known. In fact, some authors have used ψ production to de-

termine gluon distributions.[7] Thus, in general, there are many more parameters than in the present case even when one uses models like quantum chromodynamics. Also, to our knowledge, complete calculations considering all the distributions in the gluon-fusion model have not appeared in the literature. This fact, of course, does not rule out that model. But, a good point about the present model is that most of the input came from the continuum analysis and there were very few parameters. It is, of course, possible that a combination of various models could be the correct explanation.

An important set of data which will help in ruling out some of the models is the accurate determination of the angular distribution of the muons with respect to some suitable axis. This was discussed in Ref. 4 by the present author. In particular, angular distribution of the form $1+\alpha\cos^2\theta$ with very small α (in the ψ region) will strongly rule out a Drell-Yan model with light structureless quarks. CIM does give rise to smaller values of α and hence can be consistent, depending on the value of α. Another case discussed in Ref. 4 was the $\psi q\bar{q}$ vertex with structure (both γ_μ and $\sigma_{\mu\nu}$ terms). This can produce a small or zero value of α for certain values of the anomalous magnetic-moment-type term. These possible structure effects could have relevance also for the fact that we had to take large value of the pointlike coupling $g_{\psi q\bar{q}}$ (for spinless quarks) in the present case. As for the gluon-fusion model of ψ production through spin-0 χ, it was noted in Ref. 4 that the model does lead to isotropic distribution ($\alpha=0$). The present experimental status of α for ψ production is still uncertain[12,4] although $\alpha\simeq 0$ may be roughly consistent with data. In the case of ρ production, a similar experimental situation prevails.[12]

Some important further tests of this model will be in the ρ,ψ production with different incident beams such as π, $\bar{p}$, γ, etc. and also production of ω, ϕ, K^*, etc. In the present paper, the proton-proton case was considered separately because of the following reasons. First of all, the most extensive set of data exists for dilepton production in the proton-proton case. Data on other beams are only gradually becoming available. Furthermore, from the point of view of the CIM, the present case is the cleanest one in that only a limited number of diagrams enter the picture. For other beams there are other diagrams which could make the answers more model dependent. Finally, the probability functions (G's) are well determined for protons from electroproduction, neutrino data, etc. Thus, although it is desirable to extend the model to other beams, agreement with such an extensive set of data in the proton-proton reactions is by itself an indication of the validity of the model. Other processes are being considered, and we hope to discuss them later.

---

[1] R. Blankenbecler, S. J. Brodsky, and J. F. Gunion, Phys. Rev. D 6, 2652 (1972); D. Sivers, S. J. Brodsky, and R. Blankenbecler, Phys. Rep. 23C, 1 (1976).

[2] M. Duong-Van, K. V. Vasavada, and R. Blakenbecler, Phys. Rev. D 16, 1389 (1977).

[3] S. D. Drell and T. M. Yan, Phys. Rev. Lett. 25, 316 (1970).

[4] K. V. Vasavada, Phys. Rev. D 16, 146 (1977).

[5] J. F. Gunion, Phys. Rev. D 11, 1796 (1975); 12, 1345 (1976); M. B. Green, M. Jacob, and P. V. Landshoff, Nuovo Cimento 29A, 123 (1975); A. Donnachie and P. V. Landshoff, Nucl. Phys. B112, 233 (1976); H. Komatsu, Prog. Theor. Phys. 56, 988 (1976); D. I. Sivers, Nucl. Phys. B106, 95 (1976).

[6] Y. Kinoshita and K. Kinoshita, Univ. of Bielefeld Report No. BI-TP 77/11, (unpublished); H. Fritzsch. Phys. Lett. 67B, 217 (1977).

[7] M. B. Einhorn and S. D. Ellis, Phys. Rev. D 12, 2007 (1975); S. D. Ellis, M. B. Eihnorn, and C. Quigg, Phys. Rev. Lett. 36, 1263 (1976); C. E. Carlson and R. Suaya, Phys. Rev. D 14, 3115 (1976); 15, 1416 (1977); S. Nandi and H. R. Schneider, *ibid.* 18, 756 (1978); M. Gluck, J. F. Owens, and E. Reya, *ibid.* 17, 2324 (1978).

[8] Quarks are considered spinless in Ref. 2 and here. A recent paper deals with CIM with spin-$\frac{1}{2}$ quarks, and results similar to Ref. 2 are obtained. [See C. M. Debeau and D. Silverman, Phys. Rev. D 18, 2435 (1978).] Thus at least for the present purpose, the spinor nature of quarks is not essential. Spin considerations are, however, crucial for the angular distribution problem discussed in Ref. 4.

[9] This expression for σ is exact. An approximate expression valid for large s and Q^2 was given in Eq. (7) of Ref. 2. There is a typographical error in that expression. The right-hand side in the equation for $r(s,Q^2)$ should be divided by s.

[10] M. Duong-Van, Phys. Lett. 60B, 287 (1976) and private communication. The distribution has be modified at small x to agree with recent large-energy muon scattering data.

[11] A. Bamberger *et al.*, Nucl. Phys. B134, 1 (1978). This paper gives compilation of data on $\sigma(\psi)$ vs w.

[12] J. J. Aubert *et al.*, Phys. Rev. Lett. 33, 1404 (1974); Y. M. Antipov *et al.*, Phys. Lett. 60B, 309 (1976); K. J. Anderson *et al.*, Phys. Rev. Lett. 37, 799 (1976), and contribution to Tbilisi Conference, 1976 (unpublished); F. W. Büsser *et al.*, Phys. Lett. 56B, 482 (1975); J. M. Cobb *et al.*, *ibid.* 68B, 96 (1977); H. D. Snyder *et al.*, Phys. Rev. Lett. 36, 1415 (1976); B. C. Brown *et al.*, Fermilab Report No. 77/54, 1977 (unpublished); J. G. Branson *et al.*, Phys. Rev. Lett. 38, 1331 (1977); M. Binkley *et al.*, *ibid.* 37, 574 (1976).

[13] D. M. Kaplan *et al.*, Phys. Rev. Lett. 40, 435 (1978);

Washington-Tufts-Michigan-Northeastern Univ. Collaboration experiment (private communication from Dr. J. Rutherfoord); V. Barger and R. J. N. Phillips, Phys. Lett. 73B, 91 (1978); E. L. Berger, Argonne Report No. ANL-HEP-PR-78-12 (unpublished).

[14]G. R. Farrar, Nucl. Phys. B77, 429 (1974); V. Barger, T. Weiler, and R. J. N. Phillips, *ibid.* B102, 439 (1976).

[15]D. Antreasyen *et al.*, Phys. Rev. Lett. 38, 112 (1977); 38, 115 (1977).

[16]K. Bockmann, invited talk at the Conference on Multiparticle Production Processes and Inclusive Reactions at High Energies, Serpukhov, 1976 (unpublished). This paper give a compilation of data on $\sigma(\rho^0)$ vs s and $d\sigma(\rho)/dy$ vs y and empirical fits to various distributions. S. Nandi, V. Rittenberg, and R. Schneider [Phys. Rev. D 17, 1336 (1978)] give quark-fusion-model fits for small-Q_T spectra in the case of ρ production with π, K, and γ beams.

[17]H. J. Lipkin, Fermilab-Conf-76/98-THY, 1976 (unpublished).

[18]Possibility of such variation has been also mentioned by Y. Kinoshita and K. Kinoshita (Ref. 6) and Donnachie and Landshoff (Ref. 5) in a somewhat similar context. The authors of the first paper in Ref. 6 give large-k_T fluctuations to the incoming partons, consider them highly spacelike and argue for such a change in the coupling. In our CIM model the incoming partons are regarded essentially on the mass shell, and large k_T fluctuations are not allowed. However, the reaction proceeds dominantly through the u-channel exchange which makes at least one of the quarks in the $\psi q\bar{q}$ vertex spacelike even if the two-body subprocess is regarded on the mass shell. Fritzsch (Ref. 6) has argued for circumventing the difficulty with the OZI rule by adopting a model where $q\bar{q}$ produce a highly virtual gluon which subsequently gives rise to a $c\bar{c}$ pair of ψ.

[19]See, for example, V. Barger and D. B. Cline, *Phenomenological Theories of High Energy Scattering* (Benjamin, New York, 1969), p. 132.

[20]J. G. Branson *et al.*, Phys. Rev. Lett. 38, 580 (1977); M. Binkley *et al.*, *ibid.* 37, 578 (1976).